Biophysical Chemistry 7 (1978) 325–338

PYRIDINE INTERACTIONS WITH PHENOLIC GROUPS IN WATER: EVIDENCE FOR HYDROGEN BONDING AND HYDROPHOBIC ASSOCIATION

A. Eugene PEKARY
Endocrinology Research Laboratory, Wadsworth VA Hospital, Los Angeles, California 90073, USA

Received 3 August 1977

Pyridine interactions with phenol, substituted phenol, tyrosine and poly(Glu^{50},Tyr^{50}) in aqueous solutions have been studied by ultraviolet (UV) difference spectroscopy, spectrophotometric pH titration, circular dichroism (CD) and proton magnetic resonance (PMR) spectroscopy. A red shift and spectral sharpening of the near-UV spectrum of phenol in water was noted at pyridine concentrations greater than 0.25 M. In addition, the spectrophotometric equivalence point for the phenol- or substituted phenol-phenolate equilibrium was increased about 0.5 pH units upon the addition of 1.0 M pyridine. PMR studies were consistent with the formation of a 1 : 1 phenol-pyridine hydrogen bonded complex. The equilibrium constant derived for this interaction, 0.6–0.7 M^{-1}, is greater than the corresponding value for phenol-acetate hydrogen bonding in water. Enhancement of the pyridine hydrogen bond interaction with Tyr within poly(Glu^{50},Tyr^{50}) was observed at pH > 12 due to a hydrophobic microenvironment produced by pyridine molecules intercalating between neighboring tyrosyl residues.

1. Introduction

Protein interactions with particular functional groups within DNA bases may be essential to the specificity of genetic repressors. Optical rotatory dispersion (ORD) and circular dichroism (CD) studies of DNA-repressor complexes have been complicated by the spectral overlap of aromatic amino acid chromophore bands with the very high optical density of DNA near 260 nm [1–3]. In addition, protein interaction with DNA usually results in some degree of base-pair reorientation with respect to the DNA axis. [4]. The resulting modification of the ORD and CD spectra for DNA may obscure the small contributions to optical activity which might be expected from electrostatic or hydrogen bonding interactions [5] between amino acid side chains and functional groups within the heterocyclic DNA bases. Proton magnetic resonance (PMR) studies of double-stranded DNA complexes with nuclear proteins at temperatures below the melting point, on the other hand, are not very useful due to the extreme PMR line broadening observed in such systems which undergo highly anisotropic motions [6,7].

The present studies focus on one of several potential interactions between amino acid side chains and DNA bases: the hydrogen bonding of tyrosyl OH protons with imino nitrogen lone pair electrons within heterocyclic compounds resembling DNA bases (Pekary, unpublished observations). Interest in this particular interaction follows, in part, from the high proportion of tyrosyl residues within the N-terminal region of E. coli lac repressor which binds to lac operator DNA [8]. Several experimental techniques have been employed in this study of the phenol hydroxyl-imino nitrogen hydrogen bond so that the shortcomings of one method might be compensated by results obtained with another.

Pyridine was selected as a model heterocyclic proton acceptor molecule for phenol, tyrosine and tyrosyl residue hydrogen bonding studies because (a) it is completely miscible with water and many nonaqueous solvents, (b) its difference spectrum with many phenols in water was found to contain a relatively narrow absorption in the 280–300 nm region at pyridine concentrations greater than 0.25 M, (c) it increases the pH

for phenolic half-ionization, (d) it is not optically active, and (e) the utility of pyridine-induced solvent shifts in PMR studies of hydroxylic compounds had been previously demonstrated for non-aqueous solvent systems [9].

The principal objectives of this study were, first, to assess the relative contributions of hydrogen bonding, electrostatic interaction and hydrophobic association to the complexation of pyridine with phenolic compounds in water and dilute aqueous buffer systems over a wide range of pH, second, evaluate the geometries of the predominant interactions, third, estimate the association constant for aqueous pyridine interaction with phenolic groups and last, determine whether these interactions can competitively interfere with the conformation-stabilizing intramolecular hydrogen bonds occurring within synthetic copolymers of tyrosine and glutamic acid.

2. Experimental

2.1. Materials

Spectroscopic quality heptane, pyridine and reagent grade phenol from Matheson Coleman and Bell, reagent grade o- and p-iodophenol and 1-methylpyridinium iodide from Eastman Kodak and reagent grade p-cresol, p-chlorophenol, p-tertbutylphenol, 1,2-dimethyl-2-silapentane-5-sulfonate (DSS), and 99+% deuterated D_2O, DCl, NaOD and pyridine-D_5 from Aldrich were used without further purification. L-tyrosine was purchased from Fischer Scientific Co. Deionized distilled water was used for aqueous solutions. Inorganic reagents and p-dioxane were supplied by the J.T. Baker Co. Copolymer L-glutamic acid: L-tyrosine HBr (1 : 1) [poly(Glu^{50},Tyr^{50})] with a molecular weight of 30,800 was purchased from Miles Laboratories. It was dissovled in and dialyzed against 0.001 M Tris, pH 6.8, before use.

2.2. Ultraviolet spectroscopy

Ultraviolet (UV) absorption spectra were taken with a dry nitrogen-purged Cary Model 14 spectrophotometer fitted with thermostating cell jackets in the sample and reference compartments. A Haake Model "F" thermostated circulating bath containing 95% ethanol and a Haake dry ice-containing heat exchanger, connected by foam rubber-insulated tygon tubing, maintained thermostat temperatures within $\pm 0.1^{\circ}C$. Difference spectra were obtained by filling: (a) the sample cell nearest the photomultiplier with a mixed phenol-pyridine solution, (b) the other sample cell with solvent, (c) the reference cell nearest the photomultiplier with pyridine sample solution diluted 1 : 1 by volume with solvent and (d) the other reference cell with a correspondingly diluted phenol sample solution.

2.3. Spectrophotometric pH titrations

Titration curves for phenol and substituted phenol in aqueous solutions containing 1.0 M pyridine or 0.025 M 1-methylpyridinium iodide were obtained with a Gilford Model 240 spectrophotometer at 22°C. pH values were measured with a Radiometer of Copenhagen pH meter equipped with a Corning model #476050 combination electrode. The measured pH of the reference buffers (pH 7 and 10) remained within ±0.02 pH units during all titration experiments. The absorbance of pyridine and 1-methylpyridinium iodide at 297 and 310 nm was constant at pH values less than 13 and 12, respectively.

Stock phenol solutions, pH < 6, were prepared immediately before use. A 3 ml aliquot was transferred to a 1 cm^2 cuvet, the optical density measured at 297 or 310 nm, and then one drop of 50% NaOH added to the cuvet with thorough mixing. The resulting pH (>12) and optical density were again measured: a portion of the cuvet sample was then removed and replaced by the same volume of the corresponding stock solution. After mixing, the pH was measured, the optical density recorded, the pH rechecked and then the cuvet sample again partially replaced with stock solution. After 12 to 14 repetitions, one drop of 0.5 M HCl was added to the cuvet and the pH (<3) and optical density recorded.

pH titration of tyrosine and poly(Glu^{50},Tyr^{50}) was performed in 0.001 M Tris containing 0.0 or 0.5 M NaCl and 0.0, 1.0 or 2.0 M pyridine using the above titration procedure. The poly(Glu^{50},Tyr^{50}) titrations were later repeated by an alternative procedure involving the preparation of a titration series (pH 6-13) 24 h prior to pH and absorbance measurements as a control for possible nonequilibrium processes.

2.4. Circular dichroism (CD) studies of poly(Glu^{50}, Tyr^{50})

CD spectra were recorded on a highly modified Beckman CD spectrophotometer interfaced with a computer of average transcients. All spectra were computer averages of 4 scans at 0.3 nm/s with a 1 s time constant and a spectral half-intensity band width of 1.5 nm or less for the near-UV and 2.0 nm for the far-UV. The far-UV spectra for poly(Glu^{50},Tyr^{50}), fig. 7, were recorded with a 2 mm pathlength cell at 25°C. The near UV CD spectra were obtained at 25°C with a 10 mm or 2 mm path cell, as indicated in fig. 8. Solution compositions are given in captions to figs. 7 and 8. CD could not be measured at optical densities greater than 2.0 due to lack of transmitted energy. CD spectra are reported as the difference in the molar extinction coefficients for left and right circularly polarized light, $\Delta\epsilon = \epsilon_L - \epsilon_R$, in M^{-1} cm^{-1}. Polymer concentrations are in terms of total amino acid residue concentration for the far-UV CD and total aromatic amino acid residue concentration for the near-UV CD [10].

2.5. Proton magnetic resonance (PMR) spectroscopy

220 MHz PMR spectra were obtained with a Varian HR-220 PMR spectrometer equipped with a Varian C-1024 time-averaging computer and variable temperature accessory. Phenol and p-cresol (1×10^{-2} M) in D_2O solutions containing 0–10 M pyridine-D_5 and 0.1% p-dioxane as internal frequency standard were prepared in 2 ml screwcap glass vials with the aid of a Gilsion Model P-200 variable volume micropipet. Reference solutions containing 0–10 M pyridine-D_5 with 0.1% dioxane and 0.1% DSS were also prepared to establish the proton chemical shift of p-dioxane relative to internal DSS. 1×10^{-2} M p-cresol-(3-6)M pyridine-D_5 solutions, with measured pD ranging from 5 to 13 were prepared by substituting increasing amounts of 20% DCl or 35% NaOD for the D_2O solvent. pD values were taken to be the observed pH reading plus 0.4, the standard correction [11]. Chemical shift and pD measurements were obtained at 17, 37 and 57°C.

Poly(Glu^{50},Tyr^{50}) which had been dialyzed against 0.001 M Tris, pH 6.8, was redialyzed extensively against distilled water before being lyophilized and then redissolved in D_2O containing 0.0 M or 1.0 M pyridine-D_5. One-half ml aliquots from each solution were pipetted into 1.5 ml polyethylene conical vials and the pD adjusted with small volumes of dilute NaOD or DCl. Each aliquot was then transferred to individual 4 mm glass NMR tubes. Following PMR spectral measurements at 17°C, the contents of each NMR tube was returned to the corresponding vial and the pD remeasured. pD values remained within ±0.2 of the initial measurement.

The PMR resonance areas of Glu β-CH_2 + γ-CH_2 (high field) and Tyr o- and m-protons (low field) for poly(Glu^{50},Tyr^{50}) were measured as previously described [7]. The proportion of observable protons in the high and low field regions was obtained by means of area reference capillaries containing DSS or formic acid in D_2O, respectively. These capillaries also served as chemical shift references.

3. Results

3.1. Ultraviolet spectroscopy

Due to the high optical density of pyridine at wavelengths less than about 280 nm, no completely unobscured near-UV spectra of phenol could be recorded in its presence. A relatively narrow phenol band at about 289 nm for pyridine concentrations >0.25 M, which coincides with the 0–0 vibronic transition of hydrogen-bonded-phenol in nonaqueous solvents, can be discerned in figs. 1–3. Apparently, phenol molecules in aqueous solutions containing pyridine are protected from the spectral "blurring" effect which results from hydrogen bond interaction with water [12].

Typical difference spectra with phenol-pyridine mixtures in unbuffered distilled water at <0.25 M pyridine consist only of the phenolate absorption because of the basicity of the pyridine molecule. Any unmodified phenol absorption component in the mixed phenol-pyridine solution cell will be fully subtracted by absorption in the unmixed reference cell. Since the phenolate absorption occurs at about 20 nm longer wavelength than the absorption of the corresponding phenol species, an *indirect* method for measuring phenol-pyridine interactions free of interfering pyridine absorption suggested itself. Why not measure the phenolate optical density versus pH in aqueous pyridine solutions and then derive the phenol-pyridine

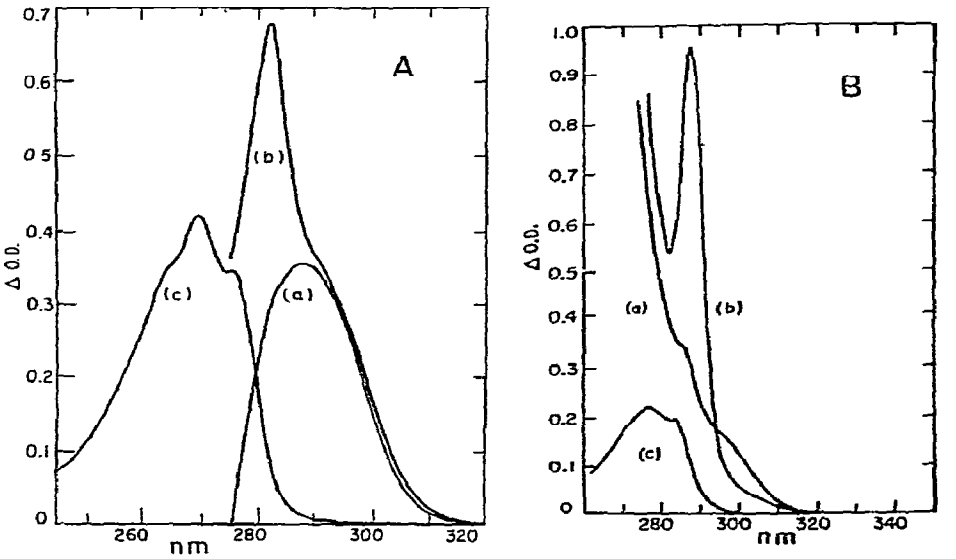

Fig. 1. (A) Difference spectrum for: (a) 3.83×10^{-3} M phenol-2.98×10^{-2} M pyridine, 5.0 cm cells, (b) 3.83×10^{-3} M phenol-1.0 M pyridine, 1.0 cm cells. (c) Spectrum for 2.79×10^{-5} M phenol, 5.0 cm cells. (B) Difference spectrum for: (a) 5.47×10^{-4} M p-tert.butylphenol-0.5 M pyridine, 5.0 cm cells, (b) 5.47×10^{-4} M p-tert.butylphenol-2.0 M pyridine, 5.0 cm cells. (c) Spectrum for 1.25×10^{-4} M p-tert.butylphenol, 1 mm cells. All spectra at 23.5°C in unbuffered distilled water.

association constants from the observed shift in the spectrophotometric equivalence point, pH_{eq}, of the phenol-phenolate equilibrium?

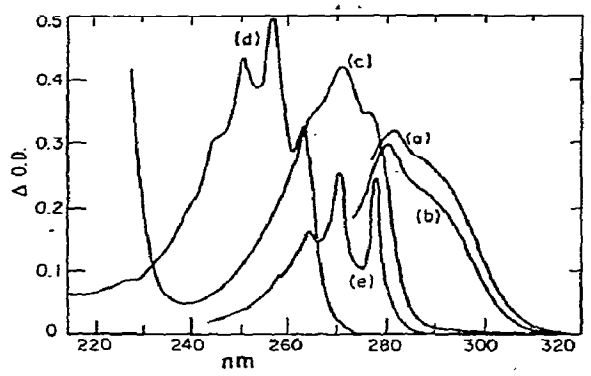

Fig. 2. Difference spectrum for: 3.8×10^{-3} M phenol-0.31 M pyridine, 1.0 cm cells, at (a) 23.5°C and (b) 0°C. Spectrum at 23.5°C for: (c) 2.79×10^{-5} M phenol, 5.0 cm cells, (d) 1.23×10^{-4} M pyridine, 1.0 cm cells. Solutions (a)–(d) in unbuffered distilled water. (e) 1.21×10^{-3} M phenol at 23.5°C in heptane, 1.0 mm cell.

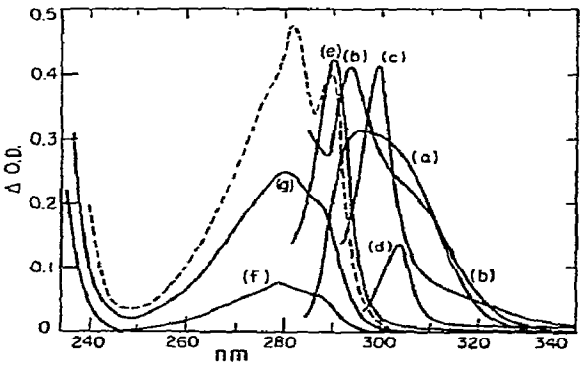

Fig. 3. Difference spectrum for: (a) 1.25×10^{-3} M p-chlorophenol-0.5 M pyridine, 21°C, 1.0 cm cells; (b) 1.56×10^{-4} M p-chlorophenol-2.0 M pyridine, 26°C, 5.0 cm cells, (c) 3.13×10^{-2} M p-chlorophenol-6.2 M pyridine, 70°C, 5.0 cm cells; (d) 3.13×10^{-2} M p-chlorophenol-12.4 M pyridine, 23.5°C, 5.0 cm cells; (e) 6×10^{-4} M p-chloroanisole-0.5 M pyridine, 0°C, 5.0 cm cells. Spectrum for: (f) 6×10^{-4} M p-chloroanisole, 23.5°C, 1.0 mm cells, (g) 1.74×10^{-4} M p-chlorophenol, 23.5°C, 1.0 cm cells. Solutions (a)–(g) in unbuffered distilled water. (———) 2.38×10^{-4} M p-chloroanisole in cyclohexane at 23.5°C, 1.0 cm cells.

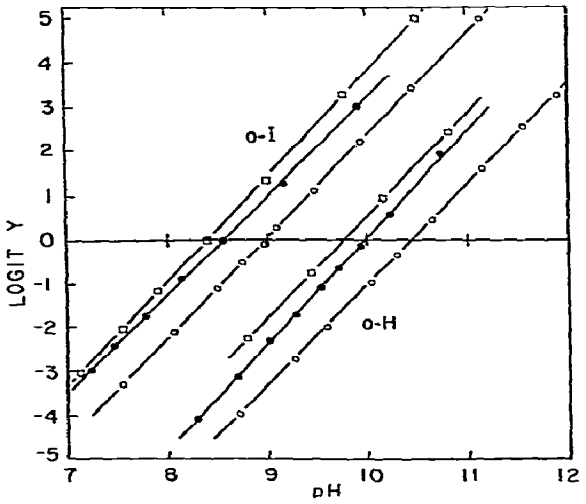

Fig. 4. Logit transformation of spectrophotometric pH titration data, obtained at 22°C, for: 9.1×10^{-4} M o-iodephenol (o-I) at 310 nm and 9.4×10^{-4} M phenol (o-H) at 297 nm in: 0.025 M 1-methylpyridinium iodide (open squares); distilled water (closed circles); 1.0 M pyridine (open circles). Logit $Y = \ln[Y/(1 - Y)]$ where $Y = \Delta A/\Delta A_0$ and ΔA_0 is the maximum change in the phenolate absorption between acidic and basic pH.

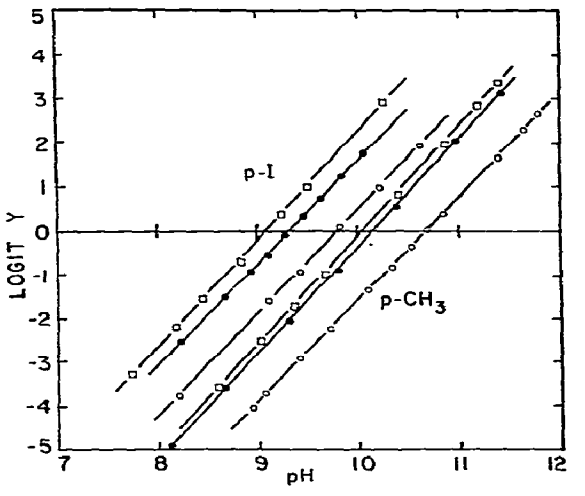

Fig. 5. Logit transformation of spectrophotometric pH titration data, obtained at 22°C, for: 1.4×10^{-3} M p-iodophenol (p-I) at 310 nm and 6.0×10^{-4} M p-cresol (p-CH_3) at 297 nm in: 0.025 M 1-methylpyridinium iodide (open squares); distilled water (closed circles); 1.0 M pyridine (open circles). Logit Y is defined in the caption to fig. 5.

3.2. Spectrophotometric pH titration

The addition of 1.0 M pyridine shifts the logit-transformed [13] spectrophotometric pH titration curves for the phenols in figs. 4 and 5 about 0.5 pH units to higher value. All phosphate and amine buffer systems examined, and even moderate ionic strengths, oppose this effect. 0.5 M phosphate buffer and 0.5 M NaCl, for example, reduce the $pH_{eq} - pK_a$ values derived from table 1 about 50% and 30%, respectively. It is interesting to note that the addition of 0.025 M 1-methylpyridinium iodide, figs. 4 and 5, *decreases* the pH at which phenol and substituted phenol half-ionization occurs. This effect is even greater for 0.025 M KI but is almost undetectable for 0.025 M KF, KCl and KBr.

The ionization behavior of tyrosine at very low ionic strengths, fig. 6A, can be distinguished from that for monosubstituted phenols, figs. 4 and 5, by the upward curvature in the logit-transformed pH titration data for this amino acid. The degree of curvature in fig. 6A is constant for tyrosine concentrations less than 6×10^{-4} M. On the other hand, the logit transform of tyrosine optical density in 0.5 M NaCl, fig. 6B, is a linear function of the measured pH.

In fig. 6C, an upward curvature, beginning at pH values greater than 12, can also be seen for the logit-transformed pH titration data of 5.2×10^{-5} M (Tyr) poly(Glu^{50},Tyr^{50}) in 0.001 M Tris. The half-titration point occurs at about 1.5 pH units above that for normal Tyr ionization [14]. Beside the expected shift of the pH titration curve to higher pH values upon the addition of 1.0 M or 2.0 M pyridine, an anomalous deviation of the linearized plot is noted at pH 12–12.5. Poly(Glu^{50},Tyr^{50}) titration in the presence of 0.5 ionic strength, fig. 6D, results in a logit-transformed pH titration curve which is linear with a half-titration point about 0.5 units above that for normal Tyr ionization. Addition of 1.0 or 2.0 M pyridine again shifts the titration curve to the right and produces an anomaly above pH 12. The deviation from linearity at high pH in the presence of 0.5 M NaCl and 2.0 M pyridine is not as pronounced as the corresponding effect observed at low ionic strengths. Nonequilib-

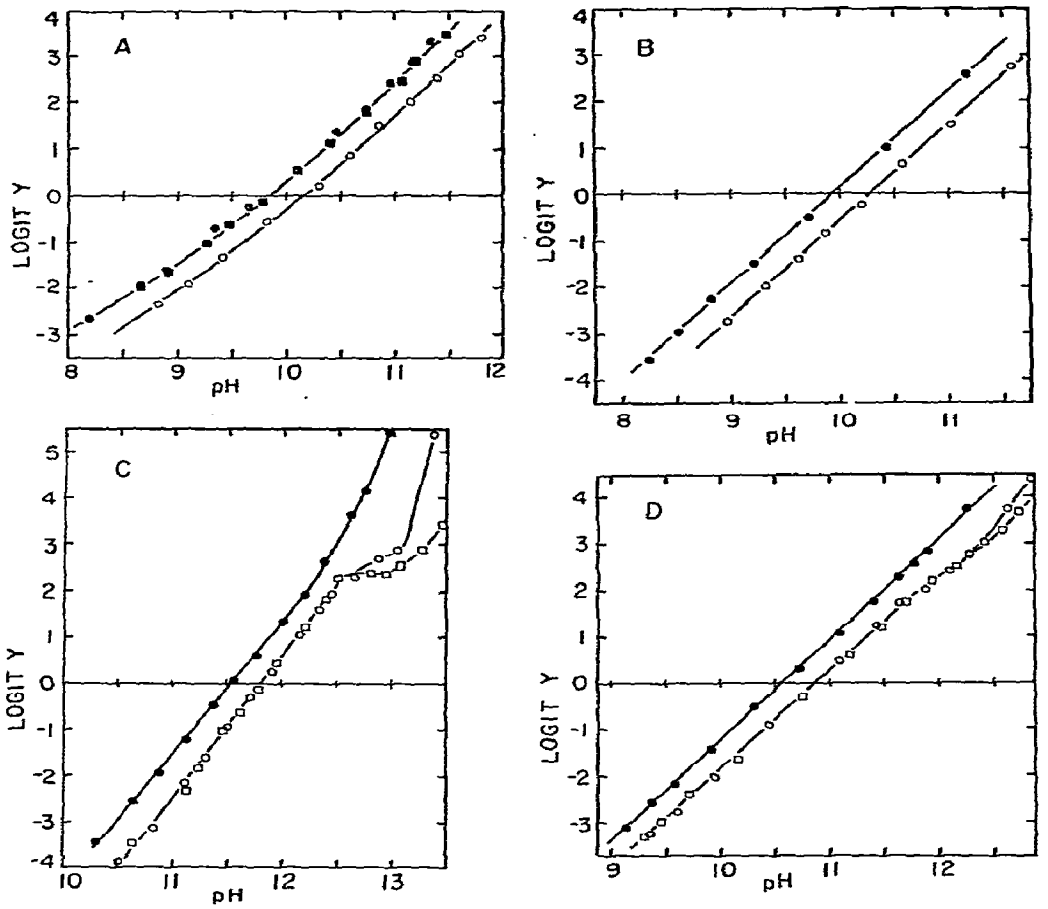

Fig. 6. Logit transformation of spectrophotometric pH titration data at 297 nm and 22°C for: (A) 6.07×10^{-4} M tyrosine (solid circles); 5.19×10^{-5} M tyrosine (solid squares) in 0.001 M Tris and 6.07×10^{-4} M tyrosine in 0.001 M Tris-1.0 M pyridine (open circles); (B) 9.18×10^{-4} M tyrosine in: 0.001 M Tris-0.5 M NaCl (solid circles) and 0.001 M Tris-0.5 M NaCl-1.0 M pyridine (open circles); (C) poly(Glu^{50},Tyr^{50}) 3.77×10^{-5} M (as tyrosine residues) in: 0.001 M Tris (solid circles); 0.001 M Tris-1.0 M pyridine (open circles) and 0.001 M Tris-2.0 M pyridine (open squares); (D) poly(Glu^{50},Tyr^{50}) 4.08×10^{-5} M (as tyrosine residues) in: 0.001 M Tris-0.5 M NaCl (solid circles); 0.001 M Tris-0.5 M NaCl-1.0 M pyridine (open circles) and 0.001 M Tris-0.5 M NaCl-2.0 M pyridine (open squares).

rium processes are not involved since measurements on solutions kept at 22°C for 24 h prior to pH and absorbance measurements were superimposable with these involving an approximate 15 min interval between titration steps.

3.3. Circular dichroism studies

The far-UV CD of poly(Glu^{50},Tyr^{50}), fig. 7, is highly dependent upon the solution ionic strength at those pH values (note fig. 6C-D) which correspond to negligible Tyr ionization. The positive 228 nm CD band which predominates at pH 8.28 and ionic strengths below 0.01 is rapidly replaced by a negative

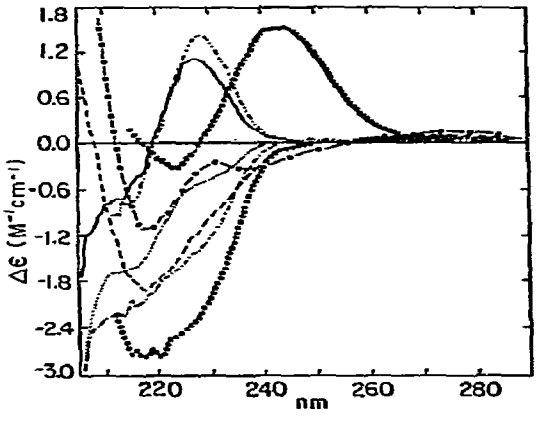

Fig. 7. Far ultraviolet circular dichroism for 8.6×10^{-4} M poly(Glu^{50},Tyr^{50}) as total amino acid concentration, at pH 8.28 and 25°C in 0.001 M Tris plus: 0.0 M NaCl (–..–..–); 0.01 M NaCl (——); 0.1 M NaCl (...); 0.25 M NaCl (–.–.–.); 0.5 M NaCl (ooo); 1.0 M NaCl (– – –); 2.0 M NaCl (–•–•–•) and at pH 13 in 0.001 M Tris plus 0.0 or 0.5 M NaCl (•••). Pathlength; 2 mm.

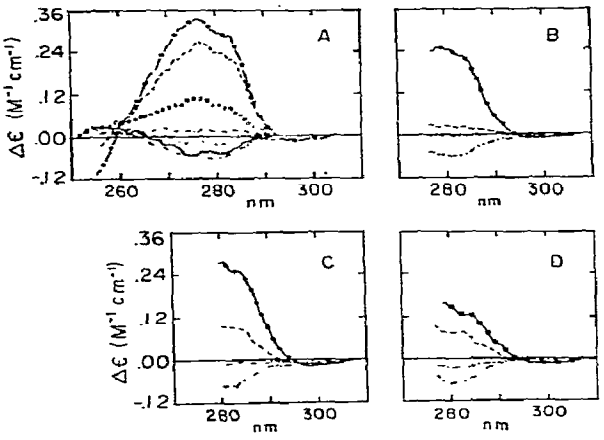

Fig. 8. (A-C) Near ultraviolet circular dichroism for 4.3×10^{-4} M poly(Glu^{50},Tyr^{50}) or (D) 2.15×10^{-3} M poly(Glu^{50},Tyr^{50}) as tyrosine amino acid residue concentration at pH 8.28 and 25°C in 0.001 M Tris plus 0.0 M NaCl (–..–..–); 0.01 M NaCl (——); 0.1 M NaCl (...); 0.25 M NaCl (–.–.–); 0.5 M NaCl (ooo); 1.0 M NaCl (– – –); 2.0 M NaCl (–•–•–•). Solutions in panels A, B, C, D contain, respectively, 0.0, 0.25, 0.5 and 1.0 M added pyridine. 10 mm and 2 mm pathlength cells were used in A-C and D, respectively.

220 nm CD band as ionic strength is increases to about 0.5. Further increase in the ionic strength leads to attenuation of the negative band at 220 nm and intensification of a positive band in the 195–200 nm region. A weak negative CD band appears at 237 nm when the ionic strength equals 2.0. The contributions of α-helix, β-sheet and unordered structure to the far-UV CD of poly(Glu^{50},Tyr^{50}), determined by the curve-resolution method of Chen et al. [15], are summarized in table 3.

The sensitivity of the poly(Glu^{50},Tyr^{50}) CD spectrum to perturbation by increasing ionic strength is lost when the bulk of its tyrosine residues are ionized in high pH buffers. This is seen most clearly in fig. 7 where a prominent CD band at 243 nm for poly(Glu^{50}, Tyr^{50}) in 0.001 M Tris, pH 13, remains completely unaffected by the addition of 0.5 ionic strength.

The effect of ionic strength on the near-UV CD of poly(Glu^{50},Tyr^{50}), seen in fig. 8A, is consistent with that observed in the far-UV. The weak negative Tyr CD band at 277 nm becomes strongly positive with increasing ionic strength provided Tyr ionization is negligible. On the other hand, no near-UV band attributable to ionized Tyr was observed for poly(Glu^{50},Tyr^{50}) at pH 13 in 0.001 or 0.5 ionic strength.

Pyridine modified the susceptibility of poly(Glu^{50}, Tyr^{50}) to ionic strength-induced changes in its near-UV CD spectrum as can be seen in fig. 8B-D. The principal effect with pyridine concentration increase from 0 to 1.0 M is a reduction in the intensity of the positive Tyr CD at ionic strengths greater than 0.25.

3.4. PMR spectroscopy of phenols

The 220 MHz PMR spectrum of 1×10^{-2} M phenol in 6 M pyridine-D_5 is reproduced in fig. 9. The doublet resonance of phenol's o-protons in D_2O is shifted monotonically about 0.54 ppm to *lower* field as the pyridine-D_5 concentration is increased to 10 M, as shown in fig. 10. A corresponding downfield shift of the o-protons in p-cresol is revealed in fig. 11. Chemical shifts for the other resonances of phenol and p-cresol are relatively unaffected by increasing pyridine concentration. Temperatures from 17 to 57°C do not significantly affect the extent of the o-proton chemical shift within p-cresol induced by increasing pyridine-D_5 concentration. Acidic pD values for p-cresol solutions at 3–6 M pyridine-D_5 concentration lead to upfield shifts in the o-

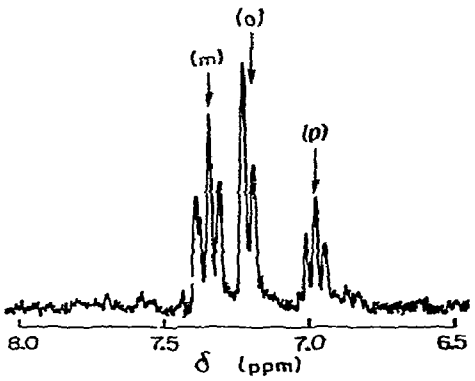

Fig. 9. 220-MHz proton magnetic resonance spectrum of 1 × 10^{-2} M phenol in 6 M pyridine-D_5 at 17°C. Center of multiplet for ortho (o), meta (m) and para (p) resonances indicated by arrows. Solvent: D_2O. Chemical shift reference: 1,1-dimethyl-2-silapentane-5-sulfonate.

proton resonance compared to the proton chemical shift observed in corresponding solutions at neutral and basic pD. The p-cresol o-proton chemical shift at acidic pD values in 3–6 M pyridine depends only on the *neutral* pyridine-D_5 concentration within these solutions as estimated from the pK_a for pyridine [16]: 5.25. This relationship coincided with the PMR data for p-cresol in *pure* D_2O solutions of increasing pyridine-D_5 concentration, fig. 11, where the *total* pyridine concentration (given in abcissa) equals the *neutral* pyridine concentration due to the basicity of these solutions.

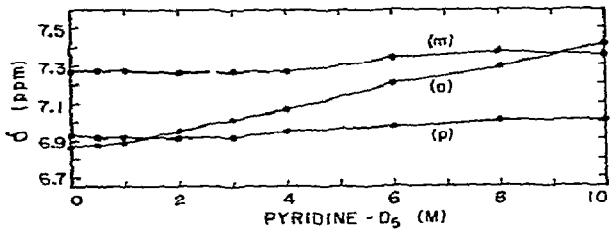

Fig. 10. Effect of pyridine-D_5 concentration on the position of 220-MHz ortho (o), meta (m), and para (p) proton magnetic resonances for 1 × 10^{-2} M phenol in D_2O at 17°C.

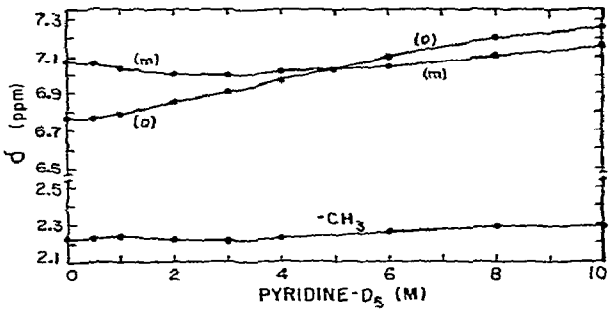

Fig. 11. Effect of pyridine-D_5 concentration on the position of 220-MHz ortho (o), meta (m), and methyl (-CH_3) proton magnetic resonances for 1 × 10^{-2} M p-cresol in D_2O at 17°C.

3.5. PMR spectroscopy of poly(Glu^{50},Tyr^{50})

The effect of 1.0 M pyridine-D_5 on the observability of proton resonances within 4.0 × 10^{-3} M (Tyr) poly(Glu^{50},Tyr^{50}) is summarized in fig. 12. The Glu (β-CH_2 + γ-CH_2) resonance visibility rises rapidly to nearly 100% as pD exceeds 11 in the presence of 1.0 M pyridine while a similar effect occurs only at pD > 13 in pyridine-free D_2O. The Tyr o- and m-proton resonances, on the other hand, are generally *less* visible in the presence of 1.0 M pyridine-D_5 than in pure D_2O. Interestingly, a *constant* 50% of the Tyr protons are

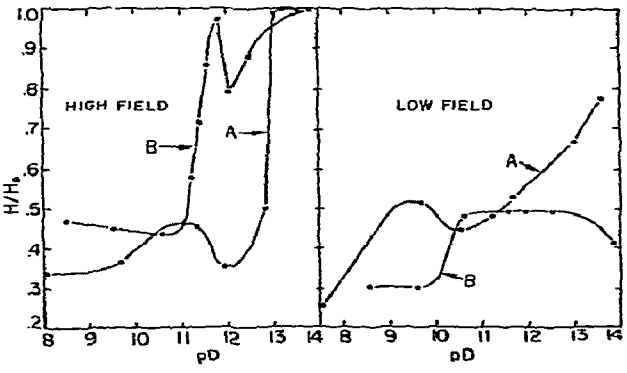

Fig. 12. Variation of proton magnetic resonance (PMR) observability with pD for poly(Glu^{50},Tyr^{50}) at 4.0 × 10^{-3} M Tyr concentration in D_2O with (A) 0.0 M and (B) 1.0 M pyridine-D_5. High field resonances correspond to Glu(β-CH_2 + γ-CH_2) and those of the low field to Tyr o- and m-protons.

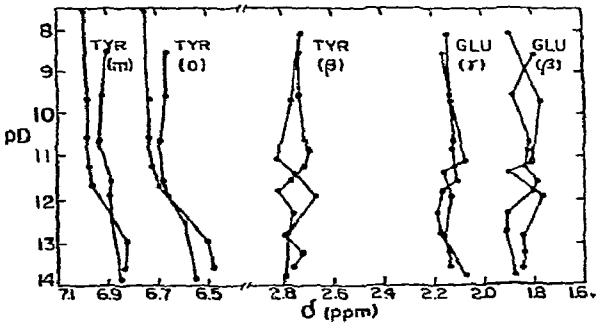

Fig. 13. Effect of pD on PMR frequencies for poly(Glu^{50}, Tyr^{50}) at 4.0×10^{-3} M Tyr concentration in D_2O with 0.0 M (–●–●–●) and 1.0 M (–o–o–o) pyridine-D_5.

visible at pD values between 10.5 and 12 in 1.0 M pyridine-D_5 while the corresponding resonances in pure D_2O increase in visibility with pD.

The PMR chemical shift versus pD profile for poly(Glu^{50},Tyr^{50}) in pure D_2O and 1.0 M pyridine-D_5 is displayed in fig. 13. A monotonic shift of the Tyr o- and m-proton resonances to *higher* field with increasing pD is clearly detectable in the absence of pyridine-D_5. 1.0 M pyridine-D_5 tends to reduce the magnitude of these shifts, particularly for Tyr o-protons. At pD < 12 the Tyr o- and m-proton resonance bands occur at higher field in 1.0 M pyridine-D_5 compared to the corresponding peaks observed in pure D_2O. Note, in figs. 10 and 11, that 1.0 M pyridine-D_5 has only a *negligible effect* on the chemical shifts within phenol and p-cresol.

The mean Tyr β-CH_2 PMR frequency variation with pD appears more complex than that seen with the Tyr o- and m-protons. In the absence of pyridine, a gradual decrease in the resonance field is observed up to pD 11. An abrupt shift to higher field occurs in the 11–12 pD range coincident with the *decrease* in PMR band visibility for Glu illustrated in the left panel of fig. 12. From pD 12-13 the Tyr β-CH_2 resonance field declines as the Glu (β-CH_2 + γ-CH_2) H/H_0 ratio in fig. 12 rises rapidly to 100% visibility. With 1.0 M pyridine-D_5, nearly reversed patterns of Tyr β-CH_2 frequency shift and Glu PMR visibility changes with pD increase are noted in figs. 13 and 12, respectively.

4. Discussion

4.1. Ultraviolet spectroscopy

The relatively featureless near-UV spectrum of phenol in water, fig. 1Ac, contrasts with the well-resolved ^1L_b progression seen in heptane, fig. 2e. This characteristic vibrational broadening effect of aqueous solvents on the UV absorption pattern of phenols has been attributed to the solvent polarity [17] and the inability of the solvation cage surrounding the chromophore to reorient during the life-time of the Franck–Condon excited state [18].

Polarization of the phenolic OH group by hydrogen bonding to pyridine increases the extent of oxygen lone-pair interaction with the π-electrons of the aromatic ring [19,20]. The magnitude of the resulting intensification of phenol's UV absorption spectrum, figs. 1Ab and 1Bb, depends on the strength of the hydrogen bond formed [21]. The pyridine-induced wavelength shift, fig. 1Ab and 1Bb, varies proportionately with the concentration of perturbant. The linearity of the phenol spectral shift with pyridine concentration increase is well illustrated in figs. 3b–d. Contributions of refractive index, dielectric constant, solvent polarizability and hydrogen bond strengths to this displacement effect have been discussed [22–25].

4.2. Spectrophotometric pH titration

The shift of the phenolic half-ionization point to higher pH values, induced by 1.0 M pyridine, relative to that measured in the corresponding aqueous solvent, figs. 4–6, illustrates another aspect of pyridine's ability to perturb phenolic hydroxyl interactions. Pyridine concentrations up to about 1.0 M do not affect the vapor pressure of distilled water significantly [26]. Thus the observed shift of about +0.5 pH units cannot be attributed to a general reduction in the water activity. In the absence of phenol interactions with pyridine the spectroscopic and acid-base properties of phenol dissolved in 1.0 M pyridine should coincide with similar results obtained in buffer alone.

The displacement of the ionization curve must be due, at least in part, to phenol hydrogen bonding with pyridine, since buffering with 0.5 M phosphate ions, which also form contact hydrogen bonds with phenol [27], reduces this effect substantially. Sodium or po-

Table 1
pK_a values for phenols in distilled water and their pH at spectrophotometric half-titration, pH_{eq}, in 1.0 M pyridine at 23°C.

Phenol	Concentration (M)	pK_a [a]	pH_{eq} [a]
phenol	9.40×10^{-4}	9.99	10.44
p-cresol	6.00×10^{-4}	10.13	10.65
o-iodophenol	9.07×10^{-4}	8.56	8.99
p-iodophenol	1.36×10^{-3}	9.39	9.84

a) Activity coefficient corrections [39] to pK_a and pH_{eq} are less than the measurement error of ± 0.02 pH units and have been omitted.

tassium fluoride, chloride or bromide do not affect significantly the ionization of phenol, in the absence of pyridine. However, potassium iodide *reduces* the pH of phenol's half-ionization point. (Note also the effects of 0.025 M 1-methylpyridinium *iodide* in figs. 4 and 5.)

The mechanism whereby iodide ions *reduce* the apparent pK_a of phenol is not understood at present. Significant electrostatic interaction between negative phenolate and positive 1-methylpyridinium ions can be ruled out, however, since further enhancement of phenol dissociation is not observed upon the substitution of pyridinium ions for sodium of potassium cations.

4.3. Quantitation of the aqueous phenol-pyridine interaction

The sigmoidal representation of spectrophotometric titration data (linear absorption and pH scales) does not lend itself to least squares analysis. Linearization of such data, however, may result from the application of the logit transformation [13] provided that a single ionization process is occurring. We have then

$$\text{logit } Y = \ln[Y/(1-Y)] = m \cdot \text{pH} + b \,, \qquad (1)$$

where $Y = \Delta A/\Delta A_0$. ΔA_0 is the maximum change in absorbance upon titration from acidic to basic pH, m is the least squares slope and b is the least squares intercept of the logit Y versus pH regression. (The logit transformation remains useful even if multiple, overlapping ionization processes are involved since their existence becomes more readily apparent due to the resulting deviations from linearity.)

By measuring phenolate absorption at a frequency in which phenol absorbance is negligible we have

$$\Delta A/\Delta A_0 = [P^-]/P_0 \,, \qquad (2)$$

where $[P^-]$ represents the concentration of phenolate ions and P_0 the total phenol concentration. Substituting eq. (2) into eq. (1) and solving for $[P^-]$ we find

$$[P^-] = \frac{P_0 \cdot e^{m \cdot \text{pH}}}{e^{-b} + e^{m \cdot \text{pH}}} \,. \qquad (3)$$

Interactions between phenolate ions, P^-, and neutral pyridine molecules, Y, is unlikely since no difference spectrum is observed in 0.1 M NaOH. Similarly, association between neutral phenol and pyridinium cations, Y^+, is improbable since the chemical shift of phenol and p-cresol o-proton resonances, figs. 10 and 11, is dependent only on the *neutral* pyridine concentration.

Let us consider a model for the association of phenol monomer, P, and dimer, P_2, molecular species with dipole–dipole assiciated [28] pyridine molecules, Y_n, $n = 1, 2, 3, \ldots, N$

$$P_0 = [P^-] + [P] + [PY] + [PY_2] + \ldots + [PY_N] + 2[P_2] + 2[P_2Y] + 2[P_2Y_2] + \ldots + 2[P_2Y_N] \,. \qquad (4)$$

The corresponding association constants for the aqueous 1 : 1 phenol-pyridine complex, PY, the 1 : 2 phenol-pyridine complex, PY_2, and the 1 : N phenol-pyridine complex, PY_N, are

$$K_{1,1} = \frac{[PY]}{[P][Y]}; \; K_{1,2} = \frac{[PY_2]}{[PY][Y]}; \; \ldots; K_{1,N} = \frac{[PY_N]}{[PY_N][Y]} \qquad (5)$$

Similarly, the association constants for the aqueous phenol dimer, P_2, and its complexes with pyridine are given by

$$K_{2,0} = \frac{[P_2]}{[P]^2}; \; K_{2,1} = \frac{[P_2Y]}{[P_2][Y]}; \; K_{2,2} = \frac{[P_2Y_2]}{[P_2Y][Y]}; \; \ldots;$$

$$K_{2,N} = \frac{[P_2Y_N]}{[P_2Y_{N-1}][Y]} \,. \qquad (6)$$

Let us assume that the step-wise association of pyridine to monomeric phenol is equivalent to the corresponding pyridine association with the aqueous phenol dimer. Then

$$K_{1,1} = K_{2,1};\ K_{1,2} = K_{2,2}; \ldots;\ K_{1,N} = K_{2,N}, \quad (7)$$

eq. (4) becomes

$$P_0 = [P^-] + ([P] + 2K_{2,0}[P]^2) \times (1 + K_{1,1}[Y] + K_{1,2}[Y]^2 + \ldots + K_{1,N}[Y]^N). \quad (8)$$

The shift to *lower* field of the phenolic o-protons with added pyridine-D_5, figs. 10 and 11, is consistent with phenol hydrogen bonding to pyridine nitrogen lone pair electrons within the 1 : 1 phenol-pyridine complex. Other pyridine molecules interacting with this complex preferentially associate with the *pyridine* aromatic nucleus by hydrophobic and dipole–dipole facilitated "stacking" interactions as observed in x-ray studies [29,30]. If a similar plane-to-plane interaction occurred between phenol and pyridine, a significant *upfield* shift [31] in some of the proton resonances for phenol, fig. 10, and p-cresol, fig. 11, should have been detectable. (Shielding effects of pyridine-D_5 on Tyr, noted in PMR studies of poly(Glu^{50},Tyr^{50}), are discussed in subsequent sections.)

Letting $K_{1,1} = K_{1,2} = \ldots = K_{1,N}$ and solving for $K_{1,1}[Y]$ we obtain for $N \to \infty$ and $[Y] = 1.0$ M

$$K_{1,1} = 1 - ([P] + 2K_{2,0}[P]^2)/(P_0 - [P^-]). \quad (9)$$

The assumption $K_{1,1} = K_{1,2}$ is introduced here for mathematical simplicity but may be justified by the observation, below, that approximate equality holds even after this constraint is removed from the curve fitting procedure.

The phenolate ion concentration, $[P^-]$, is determined at all pH values by eq. (3) for *linear* logit-transformed pH titration data. The *free* phenol concentration, [P], can be derived from the equilibrium relationship for the proton dissociation of phenol

$$[P] = [H][P^-]/K_a, \quad (10)$$

where K_a is the dissociation constant for phenol. $[Y] \approx Y_0$ due to the great excess of pyridine used. The unknown constants for phenol-pyridine association, $K_{1,1}$, and phenol dimer formation, $K_{2,0}$, are then determined by least-squares fitting of eq. (9) to the experimental logit plots in figs. 4 and 5. The best estimates for $K_{1,1}$ and $K_{2,0}$ are summarized in table 2. A corresponding treatment of similar models for phenol-pyridine association which included phenol trimers indicated that the concentration of this higher phenol aggregate is entirely negligible at the phenol concentrations used. Other models in which phenol-pyridine and pyridine-pyridine association constants were not assumed equal led to $K_{1,1}$ and $K_{1,2}$ estimates which do not differ significantly. $K_{1,1}$ and $K_{1,2}$ represent, of course, fundamentally different interactive processes, and are expected to diverge as the temperature is raised or lowered.

Table 2
Equilibrium association constant for 1 : 1 phenol-pyridine complex formation, $K_{1,1} = [PY]/[P][Y]$ and for phenol dimer formation $K_{2,0} = [P_2]/[P]^2$ in aqueous solutions containing 1.0 M pyridine. P: phenol, Y: pyridine and P_2: phenol dimer

Phenol	Concentration (M)	$K_{1,1}$ (M^{-1})a)	$K_{2,0}$ (M^{-1})b)
phenol	9.40×10^{-4}	0.60	0
p-cresol	6.00×10^{-4}	0.69	800
o-iodophenol	9.07×10^{-4}	0.57	300
p-iodophenol	1.36×10^{-3}	0.61	450

a) Estimated standard deviation: ± 0.1 M^{-1}.
b) Estimated standard deviation: ± 100 M^{-1}.

4.4. Tyrosine and poly(Glu^{50},Tyr^{50}) ionization

Upward curvature in the low ionic strength titration data for tyrosine, fig. 6A and poly(Glu^{50},Tyr^{50}), fig. 6C, is clearly related to the increased ionic strength which accompanies increased NaOH concentration. Electrostatic repulsion between the ionized carboxyl and phenolate groups of tyrosine (pK_a for $-NH_3^+$ is 9.57 and 10.18 for -OH, respectively [32]) or the ionized Glu and Tyr of poly(Glu^{50},Tyr^{50}) is thereby reduced along with the electrostatic attraction of hydronium ions to these anionic groups which increases the apparent pK_a of the phenolate groups. These relationships become more apparent after superimposing fig. 6A with 6B and fig. 6C with 6D. The resulting composites approximate the ionization pathways for tyrosine and poly(Glu^{50},Tyr^{50}) from neutrality, at low initial ionic strength, to pH 13 and back again to neutrality, at moderate ionic strength, in the absence or presence of added pyridine.

4.5. The secondary structure of poly(Glu^{50},Tyr^{50})

The far-UV CD spectra for poly(Glu^{50},Tyr^{50}) at pH

8.28 and NaCl concentrations from 0 to 2.0 M, fig. 7, correspond in many respects to CD observations for a series of peptides [33] possessing the structure (L-Tyr-L-Ala-L-Glu)$_n$ in 0.5 M NaCl–0.02 M phosphate, pH 7.4. The tripeptide Tyr-Ala-Glu, for example, exhibits an intense positive far-UV CD band at 227 nm superimposable with the far-UV CD spectrum of poly(Glu^{50}, Tyr^{50}) in ionic strengths $\leq$0.01. The other oligopeptides (n = 3, 4, 5, 7, 9, 13) also display positive CD absorption at 227 nm but of progressively decreasing intensity. The high molecular weight ordered peptide (Tyr-Ala-Glu)$_n$ (n = 200 approx.) shows only an intense negative CD band at 220 nm coincident with the far-UV CD of poly(Glu^{50},Tyr^{50}) in 0.5 ionic strength. Conformational analysis of (Tyr-Ala-Glu)$_n$ by Ramachandran [34] indicates that the helical structure of this peptide is stabilized by side chain interactions. The phenolic groups of tyrosine residues at sequence positions i form hydrogen bonds with carboxylic groups of glutamic acid residues at positions (i – 4). The correspondence of the far-UV CD spectra for poly(Glu^{50}, Tyr^{50}) to that for (Tyr-Ala-Glu)$_n$, and the rapid increase in the PMR visibility of poly(Glu^{50},Tyr^{50}) sidechains at pD values >12, fig. 12, is consistent with other evidence [5] that helix stabilization for poly(Glu^{50},Tyr^{50}) also depends on Tyr-Glu hydrogen bonding.

The near-UV CD of Tyr within helical (Tyr-Ala-Glu)$_n$ is negative while that for poly(Glu^{50},Tyr^{50}), at ionic strengths greater than 0.25, is positive. Optical activity in aromatic side chain chromophores is not an intrinsic property. Rather, it is induced by the coupling of their transition dipole moments to static electric fields, and proximate magnetic and electric dipole transition moments [10]. Correlations between changes in the observed *near-UV* CD of poly(Glu^{50}, Tyr^{50}) and a *qualitative* conformational analysis (table 3) based on the corresponding *far-UV* CD spectra provides an indirect spectrophotometric method for analyzing the effect of pyridine on the conformations of this random copolymer.

Table 3
Effect of added ionic strength on the secondary structure of 8.4 × 10^{-4} M (total residue concentration) poly(Glu^{50},Tyr^{50}) in 0.001 M Tris at pH 8.28 and 25°C

Structure (%)	NaCl (M)					
	0.01	0.1	0.25	0.5	1.0	2.0
α-helix	3	73	85	97	86	56
β-sheet [a]	—	—	—	—	—	27
unordered	97	27	15	3	14	17

[a] A negative β-sheet contribution, amounting to no more than 5%, has been avoided by omitting the β-sheet curve from the analysis where indicated by dashed lines.

4.6. *Pyridine effect on poly(Glu^{50},Tyr^{50}) secondary conformation*

The occurrence of hydrogen bonding between the phenolic hydroxyl groups of Tyr and the carboxylic groups of Glu has been observed experimentally in a random copolymer consisting of 5% tyrosine and 95% glutamic acid residues [5]. Concurrent thermodynamic studies on the hydrogen bonding of phenol to acetate ions in water [5] led to association constant estimates of 0.47 ± 0.03 M^{-1} by fluorescence spectroscopy and 0.35 ± 0.11 M^{-1} by difference absorption spectroscopy. The correspondence of the latter phenol-acetate difference spectra to similar phenol-pyridine spectra in the present study is especially noteworthy. The higher equilibrium constant for phenol-pyridine association compared to that for phenol-acetate (table 2, this work and ref. [5]) suggest that pyridine may induce a significant conformational change in amino acid polymers which depend on tyrosine-glutamic acid side chain hydrogen bonding for stabilization of their secondary structure.

Near-UV CD experiments summarized in fig. 8 suggest that pyridine does modify the structure of poly(Glu^{50},Tyr^{50}) at pH 8.28 and >0.01 ionic strengths. In fig. 8D, for example, 1.0 M pyridine reduces the $\Delta\epsilon$ for poly(Glu^{50},Tyr^{50}) in 2.0 M NaCl to 40% of its value in the absence of pyridine. It is interesting to note that at zero added ionic strength, pyridine concentrations up to 1.0 M do not affect significantly the near-UV CD of poly(Glu^{50},Tyr^{50}).

The PMR results of fig. 12, on the other hand, demonstrate, at nearly all pD values, an enhancement of the Glu(β-CH$_2$ + γ-CH$_2$) resonance area and a relative decrease in the Tyr o- and m-proton visibility in 1.0 M pyridine-D$_5$ compared to similar PMR measurements in pure D$_2$O. Apparently, the average spatial disposition of Glu and Tyr within the random copolymer at low added ionic strength (pD < 10) is not affected by

1.0 M pyridine but the anisotropic mobility of the Glu sidechains is increased about as much as it is decreased for the phenolic rings of Tyr. Evidently, some intramolecular structure persists in this highly charged polyanion even at zero added ionic strength, provided the Tyr OH groups are not all ionized. (The *intrapolymer* ionic strength of the PMR and CD studies should be at least 0.1 due to the counterion condensation effect [35,36].)

The ability of pyridine molecules to compete with Glu sidechain carboxyl groups for association with Tyr is greatly enhanced by the partial ionization of Tyr at pD > 11, as clearly evidenced by the dramatic rise in Glu PMR visibility, seen in fig. 12, above this pD value. The instability of the pyridine-Tyr interaction, which is due to the high translational entropy of pyridine, is now partially compensated by the increased instability of the Tyr-Glu hydrogen bonding resulting from the partial ionization of Tyr.

The intrinsically greater stability of the Tyr-pyridine interactions compared to that for Tyr-Glu may be inferred from the demonstration in fig. 12 that at approximately 50% Tyr ionization (pH 11.5–12 according to fig. 6C), *all* Glu protons have sufficient rotational and vibrational mobility to be completely PMR visible while no more than one-half of the Tyr groups are detectable in the presence of 1.0 M pyridine-D_5. If the glutamic acid and tyrosyl residues within poly(Glu^{50}, Tyr^{50}) are distributed randomly within the copolymer sequence, then it is readily shown that only one-forth of the possible tetrapeptide sequences will favor intramolecular Glu-Tyr hydrogen bonding [34], while one-forth will permit interactions between adjacent Tyr's which represent 50% of the potential low field resonances. From the right hand panel of fig. 12 we see that slightly more than 25% of the Tyr resonances are visible within the pD range 8–10. Titration from pD 10 to 11 in the presence of 1.0 M pyridine-D_5 leads to an approximately one-forth increase in Tyr PMR visibility to 50% which remains constant up to pD 13.

The apparent motional "freezing" of 50% of the Tyr sidechains in 1.0 M pyridine-D_5 such that they remain PMR invisible over the *entire Tyr OH titration range*, fig. 6C, suggests that hydrogen bonding is not the only factor contributing to this phenomenon. Moreover, the electrostatic repulsion between juxtaposed Tyr residues should increase quadratically with the degree of ionization assuming their relative geometries remain fixed. That this electrostatic repulsion is normally sufficient to overcome residual Tyr-Tyr and Gly-Tyr interactions is seen in the right panel of fig. 12 where a nearly linear increase in Tyr observability to almost 80% occurs with pD increase from 10.5 to 13.85 in the *absence* of pyridine-D_5.

A counterbalancing *attractive* force between neighboring Tyr phenolic rings must be induced by pyridine even in the *absence* of Tyr OH groups. If pyridine molecules intercalate with dipole moments opposed between neighboring ionized tyrosyl residues, a partial stabilization of the electrostatic repulsion between the tyrosylate anions would result. Additional stability would be conferred by hydrophobic association. Dipole-induced-dipole and London dispersion forces should also contribute increasingly with the Tyr ionization. This model is consistent with the chemical shift data of fig. 13, which demonstrate a magnetic shielding effect of pyridine on Tyr o- and m-proton resonances at pD values up to 12. The upfield shift of the Tyr o-and m-protons during pD increase from 11.5 to 14 in fig. 13 is the result of Tyr ionization [37]. Note that the degree of Tyr ionization at a given pD value is reduced in the presence of 1.0 M pyridine-D_5.

The reduction of Tyr ionization within poly(Glu^{50}, Tyr^{50}) by 1–2 M pyridine at pH > 12, fig. 6C-D, may be the result of the pyridine intercalation between the tyrosyl residues. The effect is apparently due to water exclusion from the vicinity of the ionizable Tyr OH groups produced by the formation of plane-parallel pyridine-Tyr-pyridine "sandwiches", which would reduce the hydronium ion activity below that of the bulk solvent. Since the association constant for phenol-pyridine hydrogen bonding is very high in nonaqueous media (88 M^{-1} in n-heptane [38]), this type of interaction may also confer stability upon the Tyr OH bond, even at high measured pH, provided the microenvironment surrounding the Tyr's is sufficiently hydrophobic. That this may be a significant factor is suggested by the relatively greater deshielding effect of 1.0 M pyridine-D_5 on the Tyr o-protons noted in fig. 13 at pD > 12.5. The pH "anomaly" for Tyr ionization within poly(Glu^{50},Tyr^{50}) at 1.0 M pyridine may thus represent a concerted effect of hydrophobic association and hydrogen bonding between Tyr and pyridine resulting in a substantial increase in the apparent pK_a for Tyr ionization.

Acknowledgement

The author thanks Professor Chester T. O'Konski, Department of Chemistry, University of California at Berkeley, for provision of the Cary Model 14 spectrophotometer and accessories used in this work; Professor Sunney I. Chan, California Institute of Technology, for use of the Varian HR-220 proton magnetic resonance spectrometer, and Dr. Ernest Kay, Nuclear Medicine and Radiation Biology Laboratory, UCLA, for assistance with the circular dichroism measurements. This study was supported in part by USPHS Training Grant No. 2 T01 GM 00829 from the National Institute of General Medical Sciences (to AEP, 1966-70); USPHS Research Grant No. GM 12082 (to Professor O'Konski), and by VA Research Project 3590-02; USPHS Grant HD-7181 (to Professor Jerome M. Hershman, M.D.).

References

[1] K. Fukada, Y. Ohshima and T. Horiuchi, J. Biochem. 75 (1974) 935.
[2] J.C. Maurizot, M. Charlier and C. Helene, Biochem. Biophys. Res. Commun. 60 (1974) 951.
[3] R. Clement and M.P. Duane, Nucleic Acids Res. 2 (1975) 303.
[4] T.E. Wagner and V. Vandegrift, Biochemistry 11 (1972) 1431.
[5] A.Y. Moon, D.C. Poland and H.A. Scheraga, J. Phys. Chem. 69 (1965) 2960.
[6] A.E. Pekary, S.I. Chan, C.-J. Hsu and T.E. Wagner, Biochemistry 14 (1975) 1184.
[7] A.E. Pekary, H.-J. Li, S.I. Chan, C.-J. Hsu and T.E. Wagner, Biochemistry 14 (1975) 1177.
[8] K. Beyreuther, K. Adler, N. Geisler and A. Klemm, Proc. Nat. Acad. Sci. 70 (1973) 3576.
[9] P.V. Demarco, E. Farkas, D. Doddrell, B.L. Mylari and E. Wenkert, J. Am. Chem. Soc. 90 (1968) 5480.
[10] E.H. Strickland, Crit. Rev. Biochem. 2 (1974) 113.
[11] P.K. Glascoe and F.A. Long, J. Phys. Chem. 64 (1960) 188.
[12] G. Nemethy and A. Ray, J. Phys. Chem. 77 (1973) 64.
[13] H. Feldman and D. Rodbard, in: Principles of competitive protein-binding assays, eds. W.D. Odell and W.H. Daughaday (Lippincott, Philadelphia, 1971).p. 158.
[14] Y. Nozaki and C. Tanford, J. Am. Chem. Soc. 89 (1967) 736.
[15] Y.-H. Chen, J.T. Yang and M. Martinez, Biochemistry 11 (1972) 4120.
[16] R.C. Weast, ed., Handbook of Chemistry and Physics, 57th Edition (Chemical Rubber Company, Cleveland, 1976-77) p. D-148.
[17] N.S. Bayliss and E.G. McRae, J. Phys. Chem. 58 (1956) 1002.
[18] G.C. Pimentel, J. Am. Chem. Soc. 79 (1957) 3323.
[19] H. Baba and S. Suzuki, J. Chem. Phys. 35 (1961) 1118.
[20] D.A. Chignell and W.B. Gratzer, J. Phys. Chem. 72 (1968) 2934.
[21] J.E. Bailey, G.H. Beaven, D.A. Chignell and W.B. Gratze Eur. J. Biochem. 7 (1968) 5.
[22] D.B. Wetlaufer, J.T. Edsall and B.R. Hollingworth, J. Biol. Chem. 233 (1958) 1421.
[23] S. Yanari and F.A. Bovey, J. Biol. Chem. 235 (1960) 2818.
[24] F.A. Bovey and S. Yanari, Nature 186 (1960) 1042.
[25] H. Grinspan, J. Birnbaum and J. Feitelson, Biochim. Biophys. Acta 126 (1966) 13.
[26] M. Ewart, Bull. Soc. Chim. Belg. 45 (1936) 493.
[27] G.M. Bhatnagar, L.C. Gruen and J.A. McClaren, Aust. J Chem. 21 (1968) 3005.
[28] F.E. Harris and B.J. Alder, J. Chem. Phys. 21 (1953) 1031.
[29] K.A. Frazer and M.M. Harding, Acta Cryst. 22 (1967) 75.
[30] H.A. Hagihara, N. Yoshida and Y. Watanabe, Acta Crys B25 (1969) 1775.
[31] H. Perkampus and U. Kruger, Z. Physik. Chem. (neue folge) 55 (1967) 202.
[32] F. Yamazaki, K. Fujiki and Y. Murata, Bull. Chem. Soc Japan 38 (1965) 8.
[33] B. Schechter, I. Schechter, J. Ramachandran, A. Conwa Jacobs and M. Sela, Eur. J. Biochem. 20 (1971) 301.
[34] J. Ramachandran, A. Berger and E. Katchalski, Biopoly mers 10 (1971) 1829.
[35] G.S. Manning, J. Chem. Phys. 51 (1969) 924.
[36] C. Tanford, Physical chemistry of macromolecules (Joh Wiley & Son, Inc., 1961) pp. 457-525.
[37] C.C.K. Roberts and O. Jardetzky, Adv. Protein Chem. 24 (1970) p. 457.
[38] A.K. Chandra and S. Banerjee, J. Phys. Chem. 66 (196 952.
[39] A. Albert and E.P. Serjeant, The determination of ioni tion contants (Chapman and Hall Ltd., 1971) p. 29.